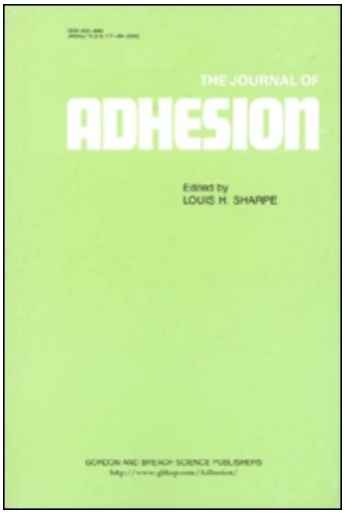

The Journal of Adhesion
Publication details, including instructions for authors and subscription information:
http://www.informaworld.com/smpp/title~content=t713453635

Fracture Markings on Stress-corroded Epoxy/Aluminum Butt Joints

W. D. Bascom[a]; S. T. Gadomski[a]; C. M. Henderson[a]; R. L. Jones[a]
[a] Surface Chemistry Branch, Naval Research Laboratory, Washington, D.C., U.S.A.

To cite this Article Bascom, W. D. , Gadomski, S. T. , Henderson, C. M. and Jones, R. L.(1976) 'Fracture Markings on Stress-corroded Epoxy/Aluminum Butt Joints', The Journal of Adhesion, 8: 3, 213 — 222
To link to this Article: DOI: 10.1080/00218467608075084
URL: http://dx.doi.org/10.1080/00218467608075084

J. Adhesion, 1977, Vol. 8, pp. 213–222

Printed in Scotland

Fracture Markings on Stress-corroded Epoxy/Aluminum Butt Joints

W. D. BASCOM, S. T. GADOMSKI, C. M. HENDERSON and R. L. JONES

Surface Chemistry Branch, Naval Research Laboratory, Washington, D.C. 20375, U.S.A.

(*Received October 8, 1975*)

Times-to-failure *vs.* static load (σ_c) in moist air and water were determined for aluminum butt-joints bonded with DGEBA-epoxy resins. A characteristic fracture marking was observed on the failed surfaces similar in shape to the mirror-markings observed on glass fracture surfaces. These markings were associated with the stress corrosion process and identified as regions of slow flaw growth originating from the bond edge. The flaw depth, r_c, and the failure stress were correlated by $\sigma_c/r_c^{\frac{1}{2}} = \text{constant}$. Fracture energies, $\mathcal{G}_c$, characteristic of the stress corrosion failure were calculated and the values obtained were in the range of 8 to 14 J/m^2 which are comparable to the threshold stress corrosion fracture energies, $\mathcal{G}_{ISCC}$, of epoxy–aluminum bonds as determined by Mostovoy and Ripling (*J. Adhesion* **3**, 145 (1971)). These results are discussed in terms of a slow flaw growth at the resin/metal boundary and an embrittlement of the material in the interfacial region.

INTRODUCTION

The moisture-induced failure of adhesive joints is well documented and recognized as a major problem in adhesive bonding technology. Despite the large amount of test data reported on the stress-corrosion of adhesive bonds relatively little is known about the micro-aspects of failure. One of the reasons for this deficiency is the difficulty in obtaining unambiguous information from post-failure examination of the fracture surfaces. Often, the areas of water attack have been obscured by corrosion products subsequently formed on the exposed metal. In other instances the surface topography is too complex to allow meaningful interpretation.

In the work described here on stress corroded butt joints of aluminum bonded with epoxy resins, it was possible to identify a surface feature

characteristic of the bond failure and to relate this fracture marking to the stress-corrosion process.

EXPERIMENTAL

Rods of aluminum alloy (2024) 2.5 cm in diameter and 13 cm long were end-bonded using the three epoxy resin compositions listed in Table I. The metal surface was milled to a 1.2 μm CLA finish and the rods were cleaned using an acid-chromate etch,[1] rinsed with tap water and air dried. The joints were assembled in a fixture similar to that described by DeLollis[2] which positioned the rod ends 0.025 cm apart. This space was filled with liquid resin by capillary flow. The specimens were heat cured as indicated in Table I. The free ends of the rods had been drilled and tapped on the longitudinal axis for loading screws. The joints were statically loaded at stresses of 25 MN/m^2 to over 70 MN/m^2 and the time-to-failure observed. In order to expose the bonded region to water or dessicant, 8 cm diameter polymethylmethacrylate (PMMA) cups were fitted around the specimens on rubber sleeves that fit snugly on the lower aluminum rod. The bond strength under linearly increasing load were determined on an Instron test machine (model TT–B) at an extension rate of 0.13 cm/min and an ambient temperature of 25$\pm$2°C. The fracture surfaces were examined using light microscopy, scanning electron microscopy (SEM, Advanced Metal Research, Model 1000) and energy dispersive x-ray analysis (EDXA, KEVEX Corp., Model 5100).

TABLE I

Epoxy[a] resin composition and cure

Curing agent	%	Cure conditions
Piperidine	5	16 hr at 120°C
Piperidine	10	16 hr at 120°C
Nadic methyl anhydride[b]	49	2 hr at 107°C 2 hr at 135°C 2 hr at 166°C

[a] Diglycidylether bisphenol A.
[b] 0.2% benzyldimethylamine.

RESULTS

The load *vs.* time-to-failure data for the 10% piperidine-DGEBA bonded specimens are plotted in Figure 1. The usual[3] exponential decrease in survival time with increasing load is evident. In these experiments the specimens were

held in ambient air (40–50% RH) or exposed to liquid water. At a given load there was no discernible difference between the failure times in air and in water. Undoubtedly, the rate of attack on the bond is different for the two conditions but this difference was hidden by the large data scatter. When the bond line was protected from ambient moisture by placing a dessicant powder (Drierite) in the PMMA cup around the bond line there was a very long increase in failure time. Under these near anhydrous conditions, the specimens survived an average of 900 hours at 72.4 MN/m^2 compared to 2 hours at 68.9 MN/m^2 in ambient air.

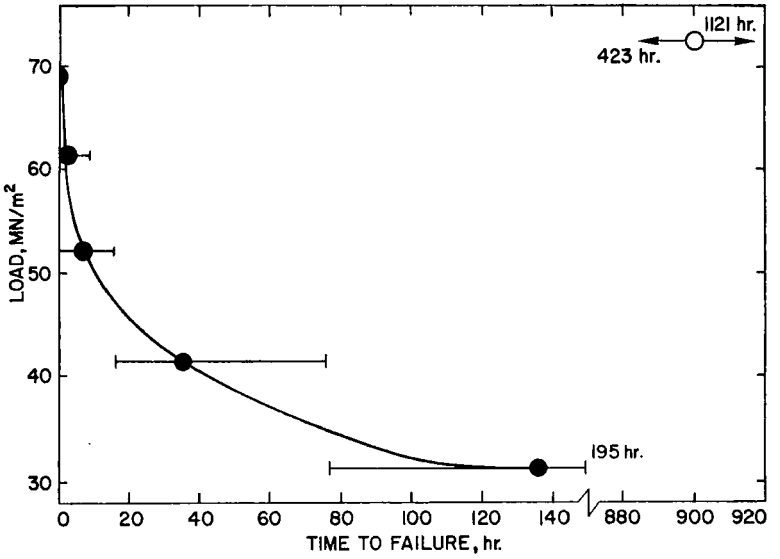

FIGURE 1 Static load *vs.* time-to-failure; ●, tested at 50% RH and in water; ○, tested in dry (<1% RH) air.

Examination of the failed surfaces revealed a fracture feature similar in shape to the mirror regions observed on glass and ceramic fracture surfaces.[4-6] Typical examples of the various butt-joint fracture surfaces are given in Figure 2. The NMA-cured resin consistently exhibited a semi-elliptical region bounded by an area of rib and hackle markings (Figure 2A). Failure in the semi-elliptical region occurred very near the resin/metal boundary (see SEM-EDXA analysis below) whereas the hackle area was center-of-bond, i.e. approximately the same amount of resin was left on both adherends. The specimens bonded with the piperidine-cured resins gave a somewhat different topography (Figure 2B) in that there was no distinct hackle region. Also, failure was close to the interface over nearly the entire bond although a film of resin could be discerned by light microscopy beyond the semi-elliptical region.

Specimens tested in the presence of the dessicant and those from the rising load tests did not exhibit the fracture markings characteristic of the tests in moist air or in water. Instead, it was possible to identify a true mirror marking; a highly reflective region of elliptical shape that had developed in the resin layer away from the interface (Figure 2C). This mirror feature was observed on all of these specimens and light microscopy examination failed to reveal any resin defects, inclusions or dust particles to be associated with the mirrors. The remainder of the fracture topography was complex and uninterpretable.

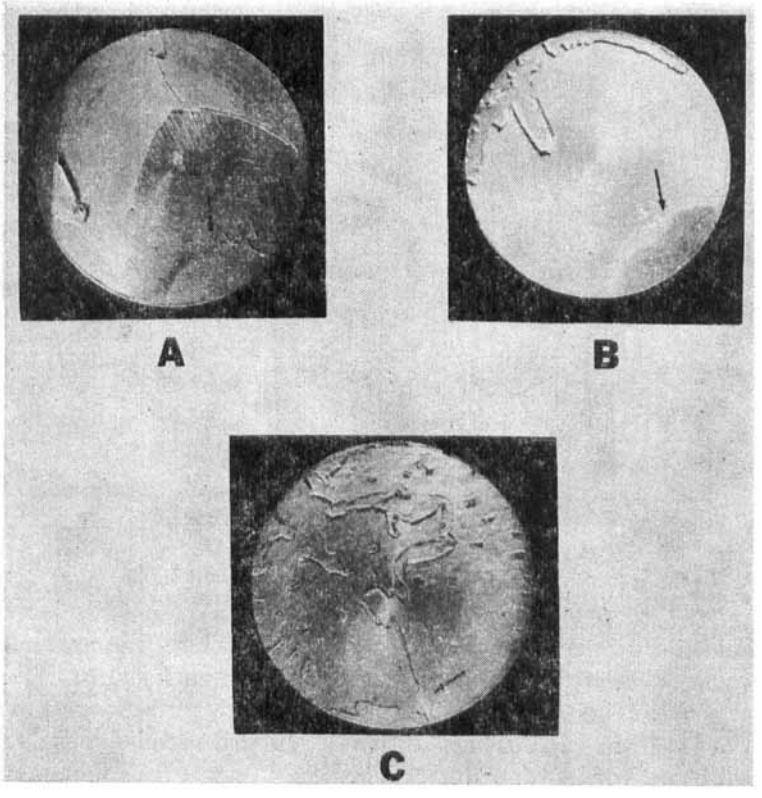

FIGURE 2 Characteristic semi-elliptical "mirror" markings on NMA–DGEBA resin (A) and piperidine–DGEBA resin (B) bonds fractured in water and an elliptical mirror on a NMA–DGEBA bond fractured in dry air (C).

Investigations of the mirror markings on brittle fracture surfaces[4-6] have established that for a given material,

$$\sigma_c r_c^{\frac{1}{2}} = \text{constant} \tag{1}$$

where σ_c is the breaking stress and r_c is the mirror "radius" taken as the distance from the specimen edge to the point of maximum penetration. A similar correlation was obtained here for the mirror-like feature on the stress-corroded butt-joint. The results for the 10% piperidine-DGEBA bonded specimens are given in Table II for different stress levels. The $\sigma_c r_c^{\frac{1}{2}}$ values are reasonably constant although the standard deviation is rather large. Equation (1) is actually for an infinite plate and its use here is of course an approximation. However, the variation in the constant term was only about 12% over a 50% variation in load. The average values of the constant of Eq. (1) for the three resin compositions are listed in Table III. Any differences between these systems are within the standard deviation of the measurements.

TABLE II

The effect of load on $\sigma_c r_c^{\frac{1}{2}}$ for the DGEBA-10% piperidine bonds

Static failure load, MN/m²	Number of specimens	$\sigma_c r_c^{\frac{1}{2}}$ MN/m$^{\frac{3}{2}}$
31.0	8	0.91±0.076
37.2	1	0.82
41.4	4	0.99
52.0	2	0.89
61.5	5	1.04±0.14

TABLE III

Fracture parameters for the butt-joints ($\sigma_c r_c^{\frac{1}{2}}$, $\mathcal{G}_c$) and the resins ($\mathcal{G}_{Ic}$)

Resin	$\sigma_c r_c^{\frac{1}{2}}$, MN/m$^{\frac{3}{2}}$	$\mathcal{G}_c$, J/m²	$\mathcal{G}_{Ic}$, J/m²
5% piperidine–DGEBA	0.790±0.111	9.0	121[a]
10% piperidine–DGEBA	0.931±0.114	12.6	—
NMA–DGEBA	0.743±0.162	8.9	124[b]

[a] Ref. 14.
[b] W. D. Bascom and R. L. Cottington, unpublished results.

The fracture surfaces were examined using SEM and EDXA. Photomicrographs of the surface near a semi-elliptical marking are given in Figure 3 for a specimen bonded with the NMA-DGEBA resin. At low magnifications (Figures 3A and 3B) three regions can be identified; an area of near interfacial failure that can be seen at high magnification in Figure 3C, an intermediate region where failure was clearly in the resin and on which there were rows of parabolic markings as shown in Figure 3D, and an area of

fracture which was essentially center-of-bond and exhibited rib and hackle markings. The interfacial region and the intermediate region cannot be readily distinguished when viewed using light microscopy and so it was necessary to include both in the measurement of r_c. Surface analysis using EDXA in the interfacial region on the resin side of the fracture failed to show a continuous coating of aluminum (oxide) or even a significant discontinuous coverage. Evidently, failure had occurred in or extremely close to the interface and followed the surface roughness so closely as to give a detailed replication of the mill marking on the metal. The reason for not calling this region an interfacial failure is that separation could have been a few hundred angstroms either side of the interface and left a layer of metal oxide or resin undetectable using EDXA analysis. Examination of the "interfacial" region of failure revealed occasional islands of resin that appear to have failed by a ductile yielding (Figure 3C) as if the corrosion process had progressed around

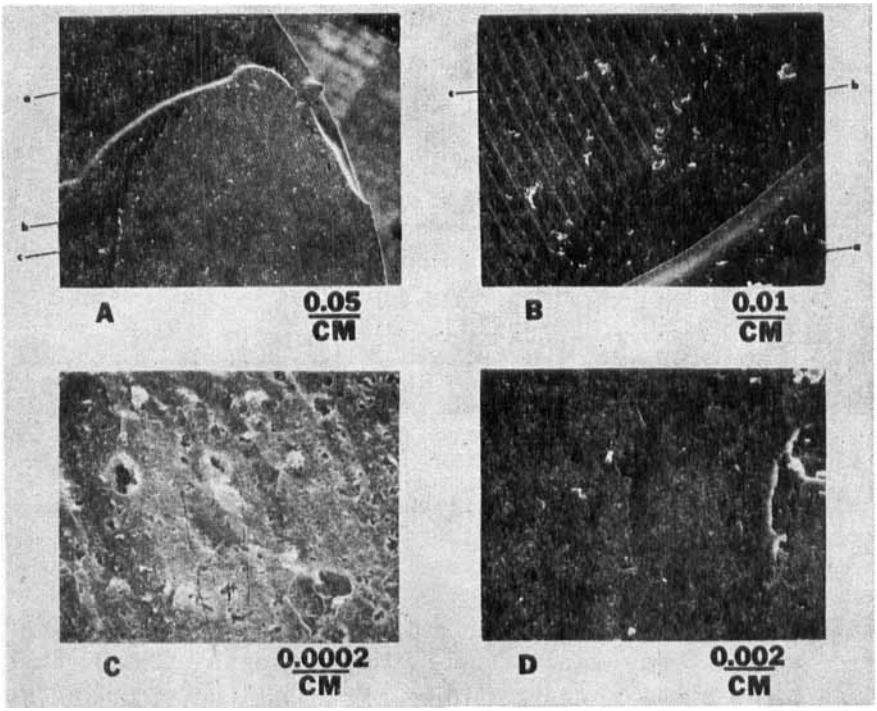

FIGURE 3 SEM photographs of a hemispherical mark on an NMA–DGEBA bond fracture surface. (A and B), low magnification views of the hackle (a), intermediate (b) and interfacial (c) regions; (C and D), high magnification views of the interfacial and intermediate regions respectively.

a small area leaving a column of resin that subsequently failed as the crack advanced.

In the intermediate region the plane of failure appeared to have moved from the interface into the resin to give a smooth fracture surface except for rows of parabolic markings (Figure 3D). Fracture parabolas are usually associated with the intersection of the main crack front with micro-cracks formed ahead of the crack.[7] The rows of parabolas were coincident with the peaks of the mill grooves as if micro-crack formation were associated with some specific interaction of the crack front stress field with the surface asperities. The presence of these parabolas is evidence that this is a region of unstable, fast crack propagation.

DISCUSSION

There is little doubt that the semi-elliptical features observed on the fracture surfaces of the static loaded specimens are associated with moisture-induced failure and represent a region of slow flaw growth. Such features were not detectable on the surfaces that failed in the presence of the dessicant or in the rising load tests. Moreover, there was a systematic increase in the "mirror" radius with the time-to-failure which of course is implied from Figure 1 if $\sigma_c/r_c^{\frac{1}{2}}$ is constant.

The $r^{-\frac{1}{2}}$ dependence of the failure stress implies brittle fracture so that the Griffith–Irwin fracture criterion should apply, i.e.

$$\sigma_c = g\left(\frac{\mathscr{G}_c E}{r_c \pi(1-\nu)}\right)^{\frac{1}{2}} \tag{2}$$

where $\mathscr{G}_c$ is the critical strain energy release rate at fracture instability, E is the tensile modulus and ν Poisson's ratio of the aluminum and g is a numerical constant determined by specimen geometry.[8] The rationale for using E and ν of the metal in applying Eq. (2) to adhesive fracture is based on the elastic restraint imposed on the resin by the stiff, metal adherends. This point has been discussed by Orowan,[9] Ripling, Mostovoy and Corten[10, 11] and treated analytically by Arin and Erdogan.[12] The degree of restraint is a function of bond thickness but its effect in the 0.025 cm bonds of this study is negligible.[11]

An explicit form for Eq. (2) can be obtained from an expression for the stress intensity factor for circumferentially notched round tension bars[13]

$$K = 0.6\,\sigma_c\sqrt{r_c\pi} \tag{3}$$

and using the relationship

$$\mathscr{G} = \frac{K^2(1-\nu^2)}{E} \tag{4}$$

we obtain

$$\mathcal{G}_c = \frac{0.36\pi\sigma_c^2 r_c(1-\nu^2)}{E} \tag{5}$$

taking $\nu = 0.33$ this reduces to

$$\mathcal{G}_c = 0.98\,\frac{\sigma_c^2\gamma_c}{E} \tag{6}$$

Note that Eq. (3) is for a round bar with a circumferential cut which for present purposes is a sufficiently good approximation of a bar with a semi-elliptical notch.

Fracture energies ($\mathcal{G}_c$, strain energy release rates) calculated for the butt-joint tests using (6) are considerably lower than the bulk or adhesive fracture energies of the resins determined in double cantilever beam fracture tests. In Table III the $\mathcal{G}_c$ values are listed in column 3 and are more than an order of magnitude lower than the $\mathcal{G}_{Ic}$ values (column 4) obtained in opening-mode rising-load tests under dry conditions.[14] The significance of these low $\mathcal{G}_c$ values is that the joint reaches instability at a critical flaw size characteristic of a material much reduced in toughness compared to "dry" resin. In other words, the action of the water is not only one of inducing flaw growth but also an "embrittlement" of the material in the resin/metal interfacial region. Once unstable propagation has ensued in this embrittled material it is sustained even when it reaches unaffected resin because of the strain rate dependence of resin fracture and the increasing compliance of the specimen. Presumably, the embrittled region is a weak hydrated oxide formation and/or chemical degradation products of the resin. The region could not be resolved in the SEM observations or the EDXA analyses.

Mostovoy, Ripling and Bersch[13] have determined the rate of stress-corrosion cracking of epoxy-aluminum bonds using double cantilever beam specimens in which they follow stress corrosion cracking as a function of applied stress. They present their data as crack rate *vs.* strain energy release rate ($\dot{a}$ *vs.* $\mathcal{G}_I$). An example of their results is given in Figure 4. They found that $\mathcal{G}_I$ approached a limiting or threshold value, $\mathcal{G}_{ISCC}$, of about 1.75 to 17.5 J/m^2 for bonds of DGEBA-epoxy resins cured with organic amines and anhydrides. Although values of $\mathcal{G}_{ISCC}$ for bonds of the resins studied here have not been reported, work in progress[16] with piperidine-DGEBA bonds to aluminum indicate the value of $\mathcal{G}_{ISCC}$ is within the range observed by Ripling *et al.*

There is an apparent anomaly in the fact that the product $\sigma_c r_c^{\frac{1}{2}}$ (i.e., $\mathcal{G}_c$) is nearly constant over a range of failure times (Table II) yet the rate of crack growth is a function of the applied $\mathcal{G}_I$ (Figure 4). The explanation lies in the fact that in approaching the threshold fracture energy, $\mathcal{G}_{ISCC}$, the relation between crack growth rate and applied $\mathcal{G}_I$ is very steep, i.e., $\mathcal{G}_I$ is nearly independent of the crack growth rate. Indeed, it would require very precise

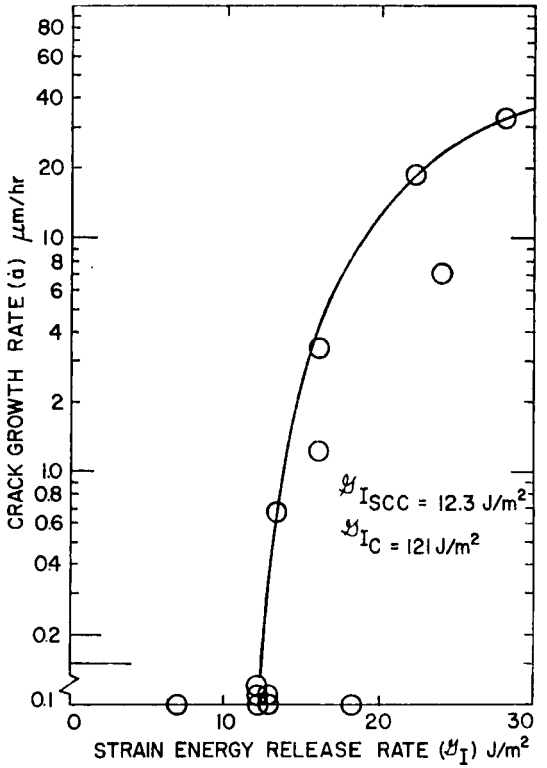

FIGURE 4 Applied $\mathcal{G}_I$ *vs.* crack growth rate for double cantilever beam specimens of aluminum bonded with hexa-hydrophthalic anhydride–DGEBA resin. Adapted from Ref. 13.

values of r_c and σ_c in order to delineate the effect of $\mathcal{G}_c$ on cracking rate in experiments of the type described here. A corollary to this fact is that simple butt-joint or lap-shear specimens in static loading can be utilized to estimate $\mathcal{G}_{ISCC}$ if the flaw size, r_c, can be determined and its relationship to σ and $\mathcal{G}$ is known. Obviously, the longer the time-to-failure (slow crack growth) the closer will the $\mathcal{G}_c$ value approach the threshold $\mathcal{G}_{ISCC}$. On the other hand, it is clear that the change in $\mathcal{G}_I$ *vs.* $\dot{a}$ in Figure 4 is too narrow to reliably predict stress *vs.* time-to-failure.

The mirror markings on the fracture surfaces of the specimens that failed with dessicant around the bond line can also be used to compute a characteristic fracture energy. These features were readily apparent as highly reflective elliptical regions on an otherwise dull resin fracture. The $\mathcal{G}_c$ was calculated from Eq. (2) from the static failure stress, σ_c, and taking one-half of the major axis of the ellipse as r_c. In a typical case with $r_c = 0.13$ cm and $\sigma_c = 72$ MN/m^2, $\mathcal{G}_c$ was 199 J/m^2 which is quite comparable to the $\mathcal{G}_{I_c}$

values of most DGEBA-resins[10, 14] and much higher than the $\mathcal{G}_{ISCC}$ for aluminum-epoxy stress corrosion. Clearly, the failure criterion under these near anhydrous conditions is the fracture energy of the resin itself.

CONCLUSION

In this study of unmodified epoxy/aluminum butt-joints in static loading, fracture energy failure criteria were derived from the failure strength, a fracture marking characteristic of the critical flaw size and the Griffith–Irwin criterion for brittle fracture. It was found that the fracture energy of these butt-joints are ten times lower than the fracture toughness of the reins itself whether the loading was in moist (50% RH) air or in water. Only in near anhydrous conditions or in rising-load tests did the failure criteria of the resin dictate joint fracture behavior.

References

1. N. J. DeLollis, *Adhesives for Metals* (Ind. Press, N.Y., 1970). P. 37.
2. Ref. 1, p. 213.
3. J. D. Minford, in *Treatise on Adhesion and Adhesives*, vol. 3, R. L. Patrick, ed. (Dekker, N.Y., 1973). P. 79.
4. E. B. Shand, *J. Amer. Ceramic Soc.* **42,** 474 (1959).
5. J. W. Johnson and D. G. Holloway, *Phil. Mag.* **14,** 731 (1966).
6. K. R. Linger and D. G. Holloway, *Phil. Mag.* **18,** 1269 (1968).
7. I. Wolock, J. A. Kies and S. B. Newman, in *Fracture*, B. L. Averback, *et al.*, eds. (Wiley, N.Y., 1954). P. 250.
8. A. S. Tetelman and A. J. McEvily, *Fracture of Structural Materials* (Wiley, N.Y., 1967). P. 50.
9. E. Orowan, in *Fatigue and Fracture in Metals*, W. M. Murray, ed. (Wiley, N.Y., 1952). P. 139.
10. E. J. Ripling, S. Mostovoy and H. T. Corten, *J. Adhesion* **3,** 107 (1971).
11. P. B. Crosley, S. Mostovoy and E. J. Ripling, *Eng. Fract. Mech.* **3,** 421 (1971).
12. K. Arin and F. Erdogan, *Int. J. Engng. Sci.* **9,** 213 (1971).
13. Arthur J. Bush, Westinghouse Research Laboratories, Pittsburgh, private communication.
14. W. D. Bascom, *et al.*, *J. Appl. Polym. Sci.* **19,** 2545 (1975).
15. E. J. Ripling, S. Mostovoy and C. Bersch, *J. Adhesion* **3,** 145 (1971).
16. W. D. Bascom and S. Gadomski, unpublished results.